2010 IEEE International Conference on Robotics and Automation
Anchorage Convention District
May 3-8, 2010, Anchorage, Alaska, USA

Design and Validation of a Multi-finger Sensing Device Based on Optical Linear Encoder

Kang Li, I-Ming Chen, Song Huat Yeo

Abstract— **This paper presents the design and validation of a wearable glove-based multi-finger motion capture device (SmartGlove) with a specific focus on the development of a new optical linear encoder (OLE). The OLE specially designed for this project has a compact size, light weight and low power consumption. The characterization tests also show that the OLE's digital output has good linearity and accuracy. The first prototype of SmartGlove which uses ten OLEs to capture the flexion/extension motion of the 14 finger joints is constructed based on the multi-point sensing method. A user study for the evaluation of SmartGlove using a standard protocol shows high repeatability and reliability in both the gripped and flat hand positions compared with four other evaluated data gloves using the same protocol.**

I. Introduction

As the intricate and prehensile parts in the body, human hands are our primary physical interaction with the world. We use our hands in varies of aspects to perform our everyday activities. Hence, monitoring and tracking human hand motion is crucial for applications in rehabilitation, skill training, entertainment, etc. In order to capture the human hand's motion, researchers have developed many sensing methods in the past few decades. Above and beyond optical [1], acoustic [2] and magnetic sensing [3], innovative techniques such as fiber-optic [4][5], strain gauge [6][7] and hall-effect sensing [8] are introduced. Nevertheless, these sensing methods still have rooms for improvement to achieve the stringent requirements from applications in medicine and skill training, such as sensing accuracy (stability of the sensor signal, repeatability & reliability of movements), ease of wear and removal, rapid calibration, adaptation for different hand sizes, no electromagnetic interference, no temperature variation, and low cost.

The paper documents the development of a new hand motion monitoring and tracking device, called SmartGlove, based on the concept of newly invented optical linear encoders (OLE) [9]. The OLE sensor, worn on the body crossing a joint (e.g., elbow, ankle, or wrist), captures body joint movement. With multiple miniature OLE sensors sticking on the back of all fingers, the finger joint movements can be captured accurately. The SmartGlove is aimed to achieve high performance hand/finger motion tracking and monitoring at an affordable cost for wide adoption. Compared to currently available hand capturing devices, the critical OLE sensing element is low-cost, compact, light-weighted, and immune to temperature or electromagnetic interferences. Ten finger OLEs form a soft exo-skeleton structure and are mounted on the glove using a quick way. The soft skeleton structure also makes SmartGlove able to fit for all hand sizes. The device can interface with general computing systems through wired and wireless standard interfaces (e.g. USB and Bluetooth). Moreover, SmartGlove can act both as a stand-alone device and as a part of a Body Sensor Network (BSN) with other OLE sensors on body joints to track entire human body movements from the hand (fine motion) to the limbs (gross motion) in a uniform interface. The novel sensing principle of SmartGlove and its relationship with hand kinamatic model are described in Section II. Prototype of the SmartGlove and system implementations is described in Section III. Calibration of the SmartGlove is discussed in Section IV. Sensor performance evaluation, in terms of repeatability, reliability and fast response and user test on the SmartGlove device as a whole are presented in Section V. The final user evaluation and performance analysis indicate that the new SmartGlove out-performs most of the current systems in terms of the given standard tasks.

Manuscript received September 14, 2009. This work was supported by the Media Development Authority, Singapore under NRF IDM004-005 Grant.

Kang Li, I-Ming Chen and Song Huat Yeo are with the Robotics Research Centre, School of Mechanical and Aerospace Engineering, Nanyang Technological University, 50 Nanyang Avenue, Singapore, 639798 (phone: 65-6790-4350; fax: 65-6793-5921; e-mail: likang@ ntu.edu.sg).

II. System Architecture

A. Multi-point Sensing Principle

The multi-point sensing principle is an extension of the single-point sensing principle proposed in the SmartSuit project [9]. The single-point OLE sensor detects joint flexion displacement through the 1-DOF linear movement of the sensor outputs. The sensor incorporates a thin encoder strip sliding in a base structure where the optical reader head acquires the movement of the strip. With the base sensor structure fixed onto one limb segment and the distal end of the encoder strip fixed to the neighboring limb segment, the sensor can interpret the linear movements of the strip caused by the joint movement as joint angles with suitable biometric data. Essentially, the OLE sensor acts like a *wearable soft exoskeleton* with sensing capability. The OLE sensor can be placed at the wrist, elbow, shoulder as well as the ankle, knee, and hip joints of different

DOFs. Two or three OLE sensors put together can detect joint motions of multiple DOFs.

The basic working principle of SmartGlove uses a variation of OLE principle by placing multiple OLEs in series on different finger segments to capture the displacements of different detecting points on a single encoder strip. This encoder strip passes through all OLEs on the same finger. Thus, it is termed as Multi-point OLE. As shown in Fig.1, three disks (from left to right) represent three in-line joints with radius of R_1, R_2 and R_3 respectively. Denote their bend angles as φ_1, φ_2 and φ_3 respectively. Three OLEs are to be placed and fixed at positions (A), (B) and (C) as shown in Fig.1. Assume the displacement readings obtained by these three OLEs are D_1, D_2 and D_3. Due to the accumulated displacement at the distal joints, we have

$$D_1 = L_1 = \frac{2\pi R_1 \varphi_1}{360} \quad (1)$$

$$D_2 = L_1 + L_2 = \frac{2\pi R_1 \varphi_1}{360} + \frac{2\pi R_2 \varphi_2}{360} \quad (2)$$

$$D_3 = L_1 + L_2 + L_3 = \frac{2\pi R_1 \varphi_1}{360} + \frac{2\pi R_2 \varphi_2}{360} + \frac{2\pi R_3 \varphi_3}{360} \quad (3)$$

Because of the natural arches of hand, the multi-point sensing can be adopted in finger motion capture. The hand has five longitudinal arches, one for each of the five digital rays. Each arch is composed of a metacarpal and its phalanges, linked by the MCP, PIP, and DIP joints. (The longitudinal arch for thumb is linked by the MCP and IP joints) [10] As introduced in the hand kinematics later, there is at least 14 joints' FE motions need to be captured in order to perform basic multi-finger sensing, and all these 14 joints are all within the five longitudinal arches. Hence, by introducing one strip for each longitudinal finger arch, it is able to use the multi-point sensing method to capture the finger's movement. In other words, multi-point sensing on a single encoding strip can be used for sensing the multiple DOF movement of an articulated object in a simple manner.

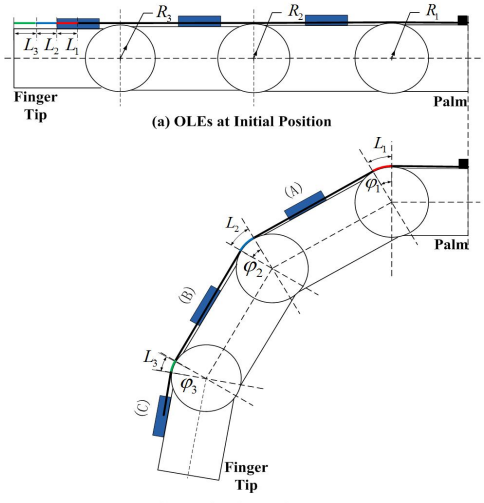

Fig. 1. Multi-point Sensing Principle.

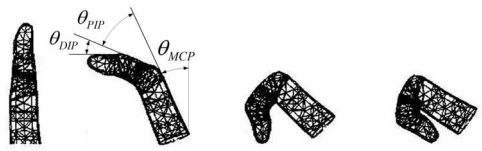

Fig. 3. Constraints between DIP and PIP joint

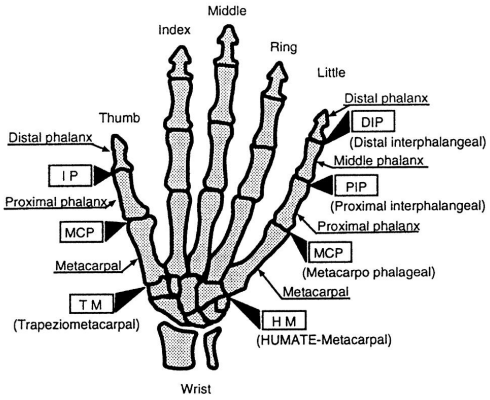

Fig. 2. Human Hand Skeleton Model.

B. Human Hand Overview

There are 23 internal degrees of freedoms (DOFs) located in the hand skeleton model (Fig.2) based on anatomical and medical analysis of the hand by previous studies and researches. [11][12] Each of the four fingers has four DOFs. The Distal Interphalangeal (DIP) joint and the Proximal Interphalangeal (PIP) joint both have one DOF and the remaining two DOFs are located at the Metacarpophalangeal (MCP) joint. Different from the four fingers, the thumb has five DOFs. There are two DOFs at the Trapeziometacarpal (TM) joint (also referred as Carpometacarpal (CMC) joint), and two DOFs at the Metacarpophalangeal (MCP) joint. The remaining one DOF of the thumb is located at the Interphalangeal (IP) joint.

The basic flexion/extension (f/e) and abduction/adduction (a/a) motions of the thumb and fingers are performed by the articulation of the above mentioned 21 DOFs. The flexion and extension motions are used to describe rotations toward and away from the palm which occurred at every joint within the hand. The abduction motion is the movement of separation (e.g., spreading fingers apart) and the adduction motion is the movement of approximation (e.g., folding fingers together). The abduction/adduction motions only occur at each finger's MCP joint as well as thumb's MCP and TM joints.

Another two internal DOFs are located at the base of the 4th and 5th (ring and little finger's) metacarpals which performs the curve or fold actions of the palm.

Although the human hand is highly articulated, it is also highly constrained. By applying those constraints, the number of DOFs in the hand can be reduced. Besides, the application of the hand motion constraints is able to synthesize natural hand motion in order to produce realistic hand animation. A commonly used one based on the hand anatomy states that for the index, middle, ring and little fingers, in order to bend the

DIP joints, the corresponding PIP joints must also be bent. (Fig.3) [13][14] The relationship can be approximately presented as:

$$\theta_{DIP} = 2/3\ \theta_{PIP} \quad (4)$$

Where θ_{DIP} refers to the flexion angle of the DIP joint and θ_{PIP} refers to the flexion angle of the PIP joint.

C. Human Hand Kinematics Modeling

Human hand is modeled with a hierarchical tree structure that consists of rigid links and joints. Each joint consists of one or two degrees of freedom. This hierarchical structure is represented in Fig.6 and each joint's position is described using D-H transformation with reference to the heel of the hand (the world coordinate system (x_0', y_0', z_0')). [15] The posture of each finger ray (labeled as 1 to 5 from the thumb to the little finger as shown in Fig.4) is represented under a local coordinate system. Now with D-H transformation, the position of each joint can be transformed from the local coordinates to the world coordinates sequentially. As shown in Fig.6, five finger rays can be divided into three different groups based on the different kinematic structure (thumb ray with five DOFs, index and middle finger rays with four DOFs, ring and little finger rays with five DOFs).

D. System Configuration

As shown in Fig. 5. The SmartGlove system consists of five multi-OLE strips (each includes two OLEs), and a microcontroller. The multi-OLE strips will send the appropriate motion data of each finger joint to the microcontroller, which will synthesize all the information sent to it from the multiple OLEs. Then, using a forward human hand kinematics model embedded into the gateway, the microcontroller will transmit the captured motion data to a remote robot, virtual reality system or computer for further analysis and application through wired or wireless communication.

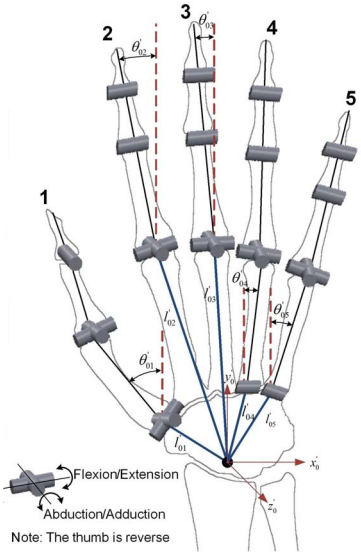

Fig. 4. Human Hand Kinematic Model

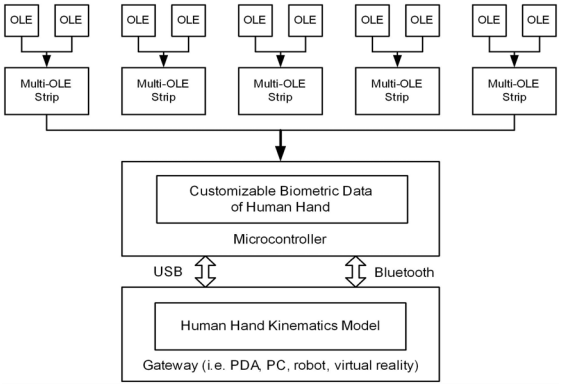

Fig. 5. System Configuration.

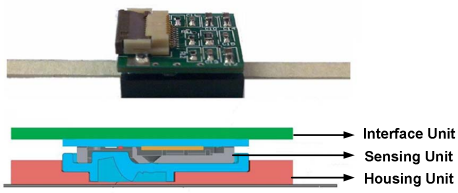

Fig. 6. OLE Module.

III. SmartGlove Prototype

A. OLE Module

The OLE module is the sensing module in the system which includes three basic units: the sensing unit (sensor and lens), the interface unit (the customized PCB board), and the housing unit (the customized base plate & strip), as shown in Fig.6. The sensing unit is fixed in the housing unit to obtain the displacement of strip and to communicate with the microcontroller through the interface unit.

The sensor used in OLE is Avago's optical mouse sensor product ADNS-3530 [16], which is based on Optical Navigation Technology that measures changes in position by optically acquiring sequential surface images (frames) and mathematically determining the direction and magnitude of movement. In order to make the size of the OLE compact, the ADNS-3530 is designed for surface mounting on a PCB board.

The housing unit is the holder for the optical navigation sensor and the moving strip made of Delrin™. According to the performance of ADNS-3530, the distance between the lens and the moving strip determines the resolution of the result. Based on the datasheet, in order to get high resolution of the sensor, the distance should be within the range of 0.77mm to 0.97mm. Furthermore, the surface material of the strip also affects the sensor's resolution. To make sure the strip sliding smoothly in the housing unit, there must be a gap between the strip and the base plate. Consequently, for the stable readout, white Formica is the ideal choice for surface material of the strip because the mean resolution is very stable within the pre-defined range.

The whole OLE module has a compact size of 13mm×12mm×4mm, and the cost is within US$50.

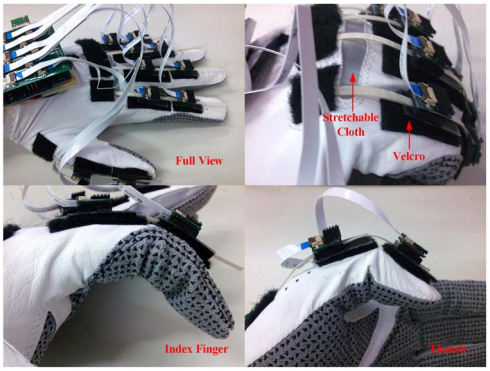

Fig. 7. SmartGlove Prototype.

B. Microcontroller

SmartGlove uses the Arduino Diecimila/Bluetooth [17] which is based on the Atmega168. It is an open-source physical computing platform based on a simple I/O board. The programming language for the Arduino microcontroller is an implementation of Wiring/Processing language. The microcontroller communicates with the OLEs via SPI protocol and sending out all the motion data to PC via USB/Bluetooth.

C. Glove Design

In this project, two different fabrics are used: the semi-stretching fabric, which can be stretched only in a single direction, and the stretching fabric, which stretches in all directions. The glove uses stretching fabric for backside of the MCP joints and semi-stretching fabric for the palm side to avoid stretching along the finger direction. Thus, the glove has good elasticity to fit the hand of users.

For ease of the replacement or maintenance of the sensors, the OLEs are mounted onto the glove using Velcro and the microcontroller connects OLEs by ribbon wires. Thus, the glove can be separated from the OLEs and all the hardware for cleaning. This feature takes a big leap toward using such data gloves in common daily living. Several photos of the SmartGlove prototype are shown in Fig.7.

IV. Calibration Method

Four simple calibration postures which are easy to perform (Fig.8) are proposed by Rachid Kadouche in order to get two approximately standard angles for each of the 10 OLEs [18].

These four calibration postures are simple and easy to perform, however, the accuracy is not good because there are only two angles (0° and 90°) for each joint to calibrate and also the joints can only approximately reach the desired degree without using external tools. Thus, a single-joint calibration, which calibrates each OLE with a specially design calibration tool with five known angles (Fig.9), is proposed in this project for more precise calibration.

By attaching each finger joint on different edges of the calibration block, four angles can be obtained. Based on these, a precise calibration for one joint can be done.

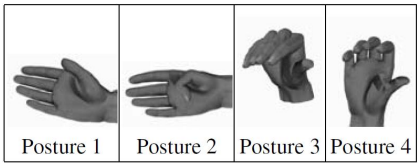

Fig. 8. Calibration Postures.

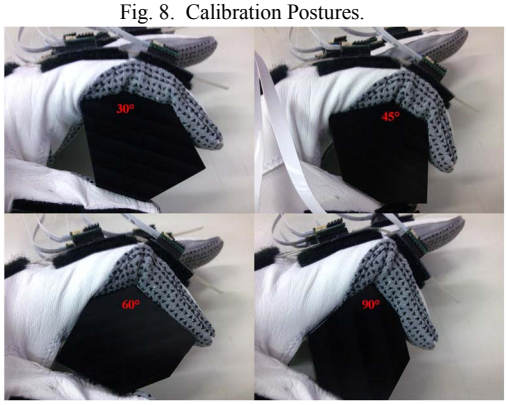

Fig. 9. Calibrate Index Finger's PIP joint using Calibration Block.

V. Preliminary Experimental Data

We performed two sets of experiments. The first set of experiments is to verify that our innovative OLE is suitable to be used in sensing human finger motion. The second set of experiments is to characterize the repeatability and reliability of the SmartGlove when ten OLEs work together.

A. OLE Characterization Test

The characterization test is carried out to evaluate the OLE on human finger.

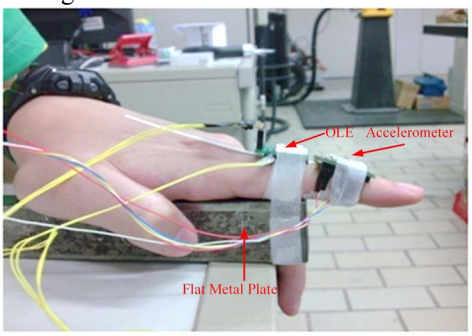

Fig. 10. Set-Up of OLE's Human Finger Test.

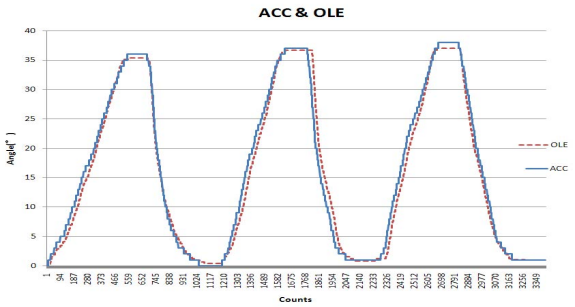

Fig. 11. Result of OLE's Human Finger Test.

The setup of the experiment is as shown in Fig.10. The OLE is attached to the first knuckle of the index finger with an accelerometer (LIS3LV02DQ from ST Microelectronics [19]) attached to the second knuckle of the index finger to measure the bending angle of the PIP joint. The palm is placed on a flat metal plate as a stable reference during the test. In the human finger test, the PIP joint of the index finger is bended back and forth three times. In the measurement, data from the OLE and the accelerometer are recorded as shown in Fig.11. Comparing the angular data from the OLE with the angular data from accelerometer (the tilt angle calculated from the three orthogonal acceleration components [20]), it is obvious that the results are very close and the difference between the linear encoder and the accelerometer is within 1°, which indicate that the OLE is suitable for human finger motion capture and can also produce good results.

B. SmartGlove Performance Tests

The evaluation procedure adopted in this project is based on the standardized evaluation protocols for sensor glove devices proposed by Wise et al. for the evaluation of Data Glove [21]. Similar tests are also adopted by Williams et al. for SIGMA Glove evaluation [22], by Dipietro et al. for Humanglove evaluation [23], by Lisa et al. for Shadow Monitor evaluation [24], and by Reinhard et al. for a sensor glove evaluation [25].

Data is collected from five healthy male students aged 22-27 years with comparable hand size and no hand movement disorders. All subjects are right-handed and the glove is placed on the right hand. Calibration using the calibration block is performed on each subject before the test.

The standardized protocols include four tests. Focusing on repeatability and reliability of multiple measurements over a single data collection session, two tests (Grip Test and Flat Test) are adopted. The Grip Test (uses a gripped hand position) and the Flat Test (uses a flat hand position) are carried out to analyze the repeatability and reliability. Five sets of measurement are performed in each test on each subject and each set of measurement includes ten grip/release actions.

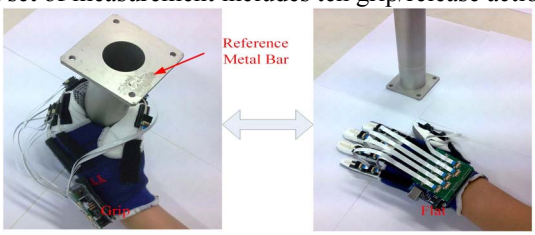

Fig. 12. Grip Test.

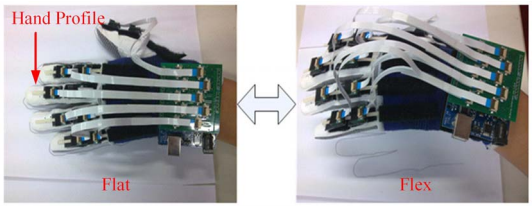

Fig. 13. Flat Test.

In the Grip Test, the subject grips the prepared cylindrical reference metal bar (with the radius of 45mm) for six seconds and then releases for six seconds (Fig.12). During the release, the subject's hand is placed flat on the table. This grip/release cycle is repeated 10 times. Repeating measurements are taken from each OLE during the grip phase. A single data block is composed of data from ten grip/release actions on one OLE. The test is repeated five times without removing the glove between successive sets, a total of 50 cycles are done.

In the Flat Test, The subject places the hand on a table and alternately raises the hand and lightly flexed the fingers, then returns the hand back to the table top (Fig.13). Each hand position lasts for six seconds and the flat/flex cycle is repeated for ten times. The repeatability of the flat hand position is explored in this test. In order to keep the hand and fingers in the same position during the flat period, an outline of the hand profile is drawn on a paper. At the flat position, the subject is asked to place the hand and fingers inside this drawn profile. The same as the Grip Test, this test is repeated five times without removing the glove between consecutive measurements and a total of 50 flex/flat cycles is done.

Repeatability is indicated by the range and standard deviation (SD), consequently, the average range and SD are obtained from each subject in each test as shown in Fig.14.

Looking into each OLE across Subjects 1 to 5 for each test, the histogram of Fig.15 summarizes the performance.

Reliability is indicated by intraclass correlation coefficient (ICC). [23] ICC analysis is performed for each test and for each OLE individually (ICC is calculated using Excel). The ICC values in Table I show consistency from one data block to another with no particular OLE showing significant lower reliability than the overall mean.

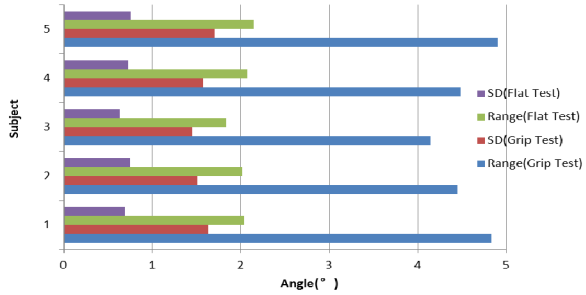

Fig. 14. Histogram of Averaged Rang and SD for Each Subject in Each Test

TABLE I
ICC OF RELIABILITY

	thumb		index		middle		ring		little		Aver -age
	MCP	IP	MCP	PIP	MCP	PIP	MCP	PIP	MCP	PIP	
Grip Test	0.937	0.954	0.882	0.963	0.913	0.987	0.948	0.957	0.969	0.964	0.947
Flat Test	0.955	0.968	0.893	0.966	0.908	0.976	0.955	0.968	0.958	0.979	0.953
Over -all											0.950

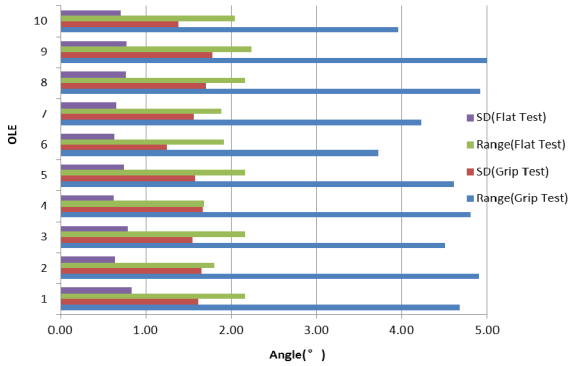

Fig. 15. Histogram of Averaged Rang and SD for Each OLE

TABLE II
COMPARISON OF RESULTS

Glove Tested	Grip Test		Flat Test		Total		ICC
	Range (°)	SD	Range (°)	Range (°)	SD	Range (°)	
Wise et al. (1990) data glove (VPL Research)	6.5	2.6	4.5	6.5	2.6	4.5	0.94
Dipietro et al. (2003) human glove (Humanware)	7.47	2.44	3.84	7.47	2.44	3.84	0.7~1.0
Simone et al. (2007) shadow monitor	5.22	1.61	1.49	5.22	1.61	1.49	0.95
Reinhard et al. (2008) WU Glove	6.09	1.94	2.61	6.09	1.94	2.61	0.93
SmartGlove	**4.56**	**1.57**	**2.02**	**4.56**	**1.57**	**2.02**	**0.95**

VI. CONCLUSION

A new hand/finger motion capturing device based on multi-point OLE sensing principle is designed and tested. The specially designed OLE for multi-point sensing has characteristics such as high resolution (can detect the strip's motion up to 20 inch/s in linear speed and 80 m/s^2 in acceleration), fast speed (at least 150Hz), low power (3.6mA), and low cost. The OLE showed good performance (accuracy within 1°compared to the accelerometer) in deployment status. Additionally, the OLE module has a compact size (13mm×12mm×4mm) and light weight (10g) which make it easy to attach to the glove to perform hand motion capture.

As shown in Table II, comparing to the previous four studies, the SmartGlove shows relatively good results in both repeatability and reliability and also lies within the measurement reliability of manual goniometry. Future research work will involve using the same OLE to sense the finger's abduction/adduction motion, increasing robustness in design, integrating other sensors, and designing applications for SmartGlove for high precision hand motion tracking.

ACKNOWLEDGMENT

This work was supported in part by the Agency for Science, Technology and Research, Singapore, under SERC Grant 0521180050, and Media Development Authority, Singapore under NRF IDM004-005 Grant.

REFERENCES

[1] W. Goebl and C. Palmer, "Anticipatory Motion in Piano Performance", *Journal of the Acoustical Society of America*, Vol.120, Issue5, pp.3004, November 2006.
[2] Power Glove User Guide, *Mattel Inc.*, September, 2007.
[3] K. Mitobe, T. Kaiga, T. Yukawa, T. Miura, H. Tamamoto, A. Rodger and N. Yoshimura, "Development of a motion capture system for a hand using a magnetic three-dimensional position sensor", *ACM SIGGRAPH Research posters: motion capture and editing*, Boston, USA, 2006.
[4] Fifth Dimension Technologies, http://www.5dt.com, 2007.
[5] Measurand Shape Advantage, http://www.measurand.com, 2007.
[6] Immersion Corporation, http://www.immersion.com, 2007.
[7] Vhand Glove, http://www.dg-tech.it/vhand/eng/, 2007.
[8] Humanware S.R.L., http://www.hmw.it/prodotti_e.html, 2008
[9] K. Y. Lim, Y. K. Goh, W. Dong, K. D. Nguyen, I.-M. Chen, S. H. Yeo, H. B. L. Duh, and C. G. Kim, "A Wearable, Self-Calibrating, Wireless Sensor Network for Body Motion Processing", *IEEE ICRA 2008*, pp. 1017-1022, Pasadena, California, May 2008.
[10] J. Lin, Y. Wu and T.S. Huang, "Modeling the Constraints of Human Hand Motion", *Proceedings of the Workshop on Human Motion, IEEE*, pp. 121-126, Los Alamitos, USA, 2000.
[11] Y. Wu and T.S. Huang, "Human Hand Modelling, Analysis and Animation in the Context of HCI", *Proceedings of the International Conference on Image Processing*. Vol.3, pp. 6-10, 1999.
[12] T. Rhee, U. Neumann and J.P. Lewis, "Human Hand Modeling from Surface anatomy", *Proceedings of the 2006 symposium on interactive 3D graphics and games*. pp. 27-34, Redwood City, California, USA, 2006.
[13] J. Lee and T.L. Kunii, "Model-Based Analysis of Hand Posture", *Computer graphics and Applications*, IEEE, Vol.15 Issue 5, pp.77-86, September 1995.
[14] J. Denavit and R.S. Hartenberg, "A Kinematic Notation for Lower-pair Mechanisms Based on Matrices", *Journal of Applied Mechanics*, ASME, Vol.22, pp.215-221, June 1955.
[15] H.-L. Yu, R. A. Chase and B. Strauch, "Atlas of Hand Anatomy and Clinical Implications", *Mosby,* 2004.
[16] Avago Technologies, http://www.avagotech.com, 2008.
[17] Arduino project, http://www.arduino.cc, 2009
[18] K. Rachid, M. Mounir, M. Marc, "Modeling of the Residual Capability for People with Severe Motor Disabilities: Analysis of Hand Posture", *International conference on user modelling*, Vol.3538, pp.231-235, Ediburgh, 2005.
[19] ST Microelectronics, http://www.st.com, 2008.
[20] W. Dong, K.Y. Lim, Y.K. Goh, K.D. Nguyen, I.-M. Chen, S.H. Yeo and B.L. Duh, "A Low-cost Motion Tracker and Its Error Analysis", *International Conference on Robotics and Automation*, pp.311-316, 19-23 May 2008.
[21] S. Wise, W. Gardner, E. Sabelman, E. Valainis, Y. Wong, K. Glass, J. Drace and J. Rosen, "Evaluation of a Fiber Optic Glove for Semi-automated Goniometric Measurements", *Journal of Rehabilitation Research and Development*, Vol.27, Issue 4, pp.411-24, 1990.
[22] N.W. Williams, J.M.T. Penrose, C.M. Caddy, E. Barnes, D.R. Hose and P. Harley, "A Goniometric Glove for Clinical Hand Assessment", *The Journal of Hand Surgery: Journal of the British Society for Surgery of the Hand*, Vol.25, Issue 2, pp.200-207, April 2000.
[23] L. Dipietro, A. M. Sabatini and P. Dario, "Evaluation of an Instrumented Glove for Hand Movement Acquisition", *Journal of Rehabilitation Research and Development*, Vol.40, Issue 2, pp.179-190, March 2003.
[24] L.K. Simone, N. Sundarrajan, X. Luo, Y.C. Jia and D.G. Kamper. "A Low Cost Instrumented Glove for Extended Monitoring and Functional Hand Assessment", *Journal of Neuroscience Methods*, Vol.160, Issue 2, pp.335-348, 2007.
[25] R. Gentner and J. Classen, "Development and Evaluation of a Low-cost Sensor Glove for Assessment of Human Finger Movements in Neurophysiological Settings", *Journal of Neuroscience Methods*, Vol.178, Issue 1, pp.138-147, March 2009.